REGOLITH MIXING IN PERMANENTLY SHADED REGIONS IN THE LUNAR SOUTH POLE, INFERRING THE DISTRIBUTION OF WATER ICE

STAR LAB

P. E. Montalvo[1] (pem0020@auburn.edu), M. Hirabayashi[1,2], and D. T. King Jr[1],

[1]Department of Geosciences, Auburn University, Auburn AL 36849 USA, [2]Department of Aerospace and Engineering, Auburn University, Auburn AL 36849 USA.

Introduction

In the lunar south pole, the major regions that host water ice materials are permanently shaded regions (PSRs) [e.g., 1–6]. The distribution of water ice may be controlled by mixing of materials, heat transfer [e.g., 7, 8], and transported and eventually cold-trapped in PSRs [e.g., 9,10,11], however these explanations may be incomplete because material in the lunar surface may be constantly mixed by impact events [12]. Cannon and Britt [13] developed a geologic model for lunar ice deposits that considers impact gardening as the primary driver that modifies the distribution of water ice and found that ice concentrations should become fairly homogeneous at meter to hectare scales in depth. Such simulations are useful to understand the evolution of regolith mixing and model at which depths water ice may reside , however they lack the spatial relationship and variation of regolith mixing depths in locations where water ice has been detected. The goal of our study is to analyze the spatial distribution of mixing process due to impact cratering events, and thus give interpretations ofwater ice deposit thickness. By obtaining the crater distributions, we can give constraints on the intensity of regolith mixing and thus the distribution of water ice present in PSRs [14-16].

Study Area

Target craters surveyed in this study are located in the lunar south pole and are located between 85˚S - 90˚S, and these include Haworth, Shoemaker and Faustini (Fig. 1). The floors of these craters are completely shadowed and host both PSRs and water ice [6]. Thus, water ice that may be stable in these areas have the potential to be mixed by constant impact cratering events at the top layer of the lunar regolith and and thus be preserved at depths.

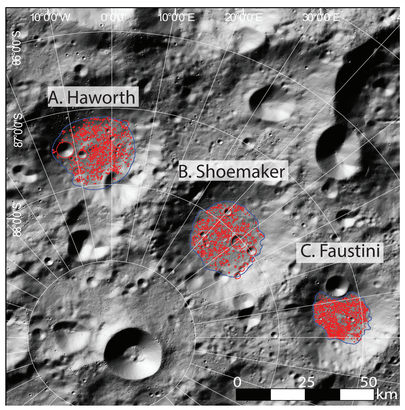

Fig. 1. Hillshade map of the lunar south pole between 85˚S - 90˚S. A. Haworth. B. Shoemaker. C. Faustini. Blue outlines indicate the counting area boundaries (crater floor). Red circles are individual crater counts.

Acknowledgements:
Supported by NASA EPSCoR grant no. 18-EPSCoR R3-0057 (Investigation of Lunar Resources) to Dr. M. Hirabayashi et al. (2019).

References: [1] Gladstone (2010) Science, 330, 472–476. [2] Hayne et al. (2015) Icarus, 255, 58–69. [3] Mandt et al. (2016) Icarus, 273, 114–120. [4] Fisher et al. (2017) Icarus, 292, 74–85. [5] Patterson et al. (2017) Icarus, 283, 2–9. [6] Li et al. (2018) PNAS, 115, 8907–8912. [7] Hayne et al. (2017) JGRP, 122, 2371–2400. [8] Stopar et al. (2017) Icarus, 298, 34–48. [9] Huang et al. (2017) JGRP, 122, 1158-1180. [10] Moores (2016) JGRP, 121, 46–60. [11] Prem P. (2015) Icarus, 255, 148–158. [12] Stopar et al. (2018) PSS, 162, 157-169. [13] Cannon and Britt (2020) Icarus, 347, 113778. [14] Prem et al. (2018) Icarus, 299, 31–45. [15] Xiao and Werner (2015) JGRP, 120, 2277–2292. [16] Hirabayashi et al. (2017) Icarus, 289, 134–143. [17] Hirabayashi et al. (2018) JGRP, 123, 527–543. [18] Kneissl et al. (2011) PI & Sp Sci, 59, 1249–1254. [19] Smith et al. (2010) Sp Sci Rev, 150, 209–241. [20] Head et al. (2010) Science, 329, 1504–1507. [21] Neukum et al. (2001) Chr Ev Mars, 96, 55-86. [22] Tye et al. (2015) Icarus, 255, 70-77. [23] Deutsch et al. (2020) Icarus, 336, 113455. [24] Wilcox et al. (2005) MAPS, 40(5), 695-710. [25] Bart et al. (2011) Icarus, 215, 485-490. [26] Fa and Wiexzorek et al. (2012) Icarus, 218, 771-787. [27] Fa et al. (2014) JGRP, 119, 1914-1935. [28] Fa et al. (2015) GRL, 42, 10179-10187.

Methods

Here, we investigate the regolith mixing depth in the lunar south polar region by using crater distributions and by applying a statistical model. We used ArcGIS CraterTools [18] and data from the Lunar Orbiter Laser Altimeter (LOLA) [19] at pixel resolutions between 5 to 20 m to perform crater counting. We performed crater counting in the crater floor of Haworth, Shoemaker and Faustini and obtained crater size frequency distributions (CSFDs) and at multiple grid sizes (2.5, 5.0 and 7.5 km) to investigate the spatial distribution of regolith mixing caused by impact cratering events. Thus, we obtain individual CSFDs at multiple resolutions. We analyzed regolith mixing depths using the technique developed by Hirabayashi et al. [16, 17]. We mapped the spatial distribution of regolith mixing depths by calculating the number of craters in a moving neighborhood [e.g., 20] of 2.5, 5.0, and 7.5 km (sampling areas of 6.25, 25, and 56.25 km²), using crater populations and modeled mixing depths. Thus, our analysis investigates the accumulation of lunar regolith thickness throughout time (e.g., the evolution of lunar regolith) by looking at the rate of crater emplacements and then calculating mixing depths. Fig. 2 shows the method's approach.

1. Process LOLA DEM using ArcGIS to produce a hillshade map
2. Count craters using CraterTools and develop measurement grids
3. Obtain CSFDs for each grid-size and crater production functions
4. Calculate mixing depths at each grid-size
5. Mapping of the spatial distribution of regolith mixing depths

Fig. 2. Flowchart of the methodology used in this study.

Results

Fig. 3 shows the crater distributions in the crater floors of Haworth, Shoemaker and Faustini. CSFDs show that the crater distribution vary in the crater floor and yield different crater productions. Obtained CPFs have slopes that range from ~3.2 to ~3.4, which are consistent with previous works [e.g., 21]. Our crater model ages are also consistent with previous crater counting statistics [e.g., 22, 23]. We calculated the regolith mixing depths (Fig. 3B-C) in the crater floors of target craters by considering the produced crater production functions (CPFs). The 90% fraction of regolith mixing ranges from ~6 m to ~18 m and varies spatially. Then we obtained CSFDs at higher resolutions by using a gridded approach. Fig. 4 shows the spatial distribution of regolith mixing at different grid sizes for each target crater (Fig. 4). The 90% area fraction of the regolith mixing greatly varies spatially by grid-size, ranging from ~1 m to ~64 m. This difference is due to individual crater population in different locations reflect higher mixing depths than the the average regolith mixing depths at the floor of each target crater.

Discussion

Our analysis shows that most of the area have consistent values compared to previous works [e.g., 24-28], however some locations yield deeper regolith mixing depths. Crater populations in those regions of higher mixing are dominated by larger craters (D > 1 km), rather than smaller craters, which would increase the mixing depth. Recently modeled mixing depths [e.g., 13] show that water ice may reside at meter to hectare scales, which is consistent with our results (Fig. 4). Our analysis indicates that lunar regolith mixing varies spatially in crater floors of target craters. It is also observable that are sensitive to the crater populations within each grid-size (Fig. 4), meaning that at higher resolutions (i.e., 2.5 km grids) lower mixing depths are seen. However, average mixing depths are consistent with coarser resolutions (i.e., 5, 7.5 km grids). Our results show that when more craters are placed, the more active the mixing process is and thus the regolith thickness is higher. Such process can mix water ice, which may have originally been on the surface, with lunar regolith throughout the impact bombardment history of craters that host water ice materials and thus be preserved at greater depths [e.g., 13]. Additionally, because water ice material is being mixed by impact gardening, impact heating processes may sublimate water ice and other volatiles present in the lunar regolith. However, they may resurface to the newly-developed cratered topography, thus newly developing lunar regolith and possibly water ice layers, thus such newly-developed water ice layers would be thin.

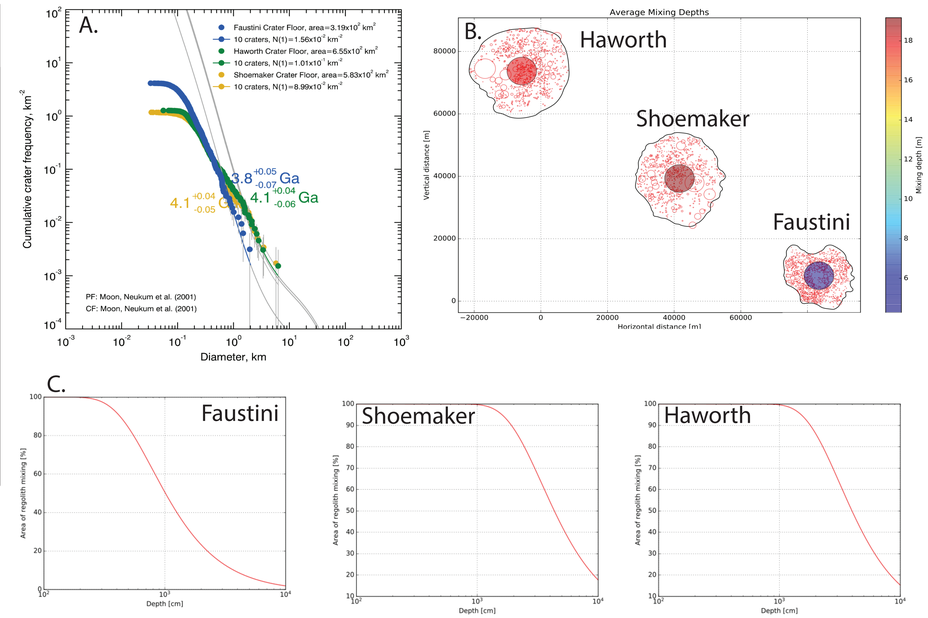

Fig. 3. Results for Haworth, Shoemaker and Faustini. A. Crater size-frequency distributions (CSFDs) of crater floors. B. Spatial distribution of average regolith mixing depths in crater floors. C. Average regolith mixing depth profiles for target craters (Faustini: ~6 m; Shoemaker: ~18 m; Haworth: ~17 m).

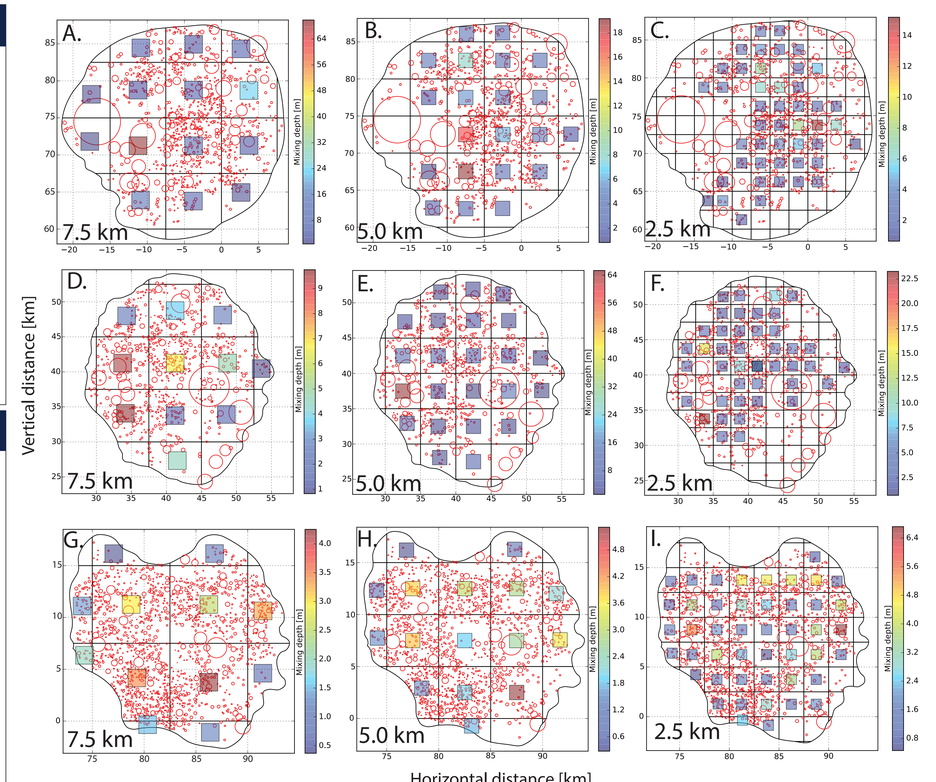

Fig. 4. Maps showing the spatial regolith mixing depths within the crater floors of target craters. A-C. Spatial regolith mixing depths in the crater floor of Haworth (~2 m to ~64 m). D-F. Spatial regolith mixing depths in the crater floor of Shoemaker (~1 m to 64 m). G-I. Spatial regolith mixing depths in the crater floor of Faustini (~0.5 m to ~6 m).